Preparation of an antibacterial poly(ionic liquid) graft copolymer of hydroxyethyl cellulose

Fanny Joubert [a,c], *R. Paul Yeo* [b,c], *Gary J. Sharples* [b,c], *Osama M. Musa* [d], *David R. W. Hodgson* [a,c,e], *Neil R. Cameron** [a,c,f,g]

[a] Department of Chemistry, Durham University, Science Laboratories, Durham DH1 3LE, UK

[b] School of Biological and Biomedical Sciences, Durham University, Science Laboratories, Durham DH1 3LE, UK

[c] Biophysical Sciences Institute, Durham University, Science Laboratories, Durham DH1 3LE, UK

[d] Ashland Speciality Ingredients, 1005 Route 202/206, Bridgewater, NJ 08807, USA

[e] Centre for Sustainable Chemical Processes, Durham University, Science Laboratories, Durham DH1 3LE, UK

[f] Department of Materials Science and Engineering, Monash University, Clayton, Victoria, 3800, Australia

[g] School of Engineering, University of Warwick, Coventry, CV4 7AL, UK

* To whom correspondence should be addressed: neil.cameron@monash.edu; +61399020774.

Keywords: Hydroxyethyl cellulose, poly(ionic liquid)s, "grafting to", RAFT polymerization, 'click' chemistry, antibacterial properties.

Abstract

Poly(ionic liquid)s (P(IL)s) of different degrees of polymerisation (10, 50 and 100) were prepared via RAFT polymerisation using an alkyne-terminated xanthate as transfer agent, with a monomer conversion of up to ~80% and a $Đ_M$ of 1.5 for $P(IL)_{100}$. Subsequently, P(IL) chains were coupled to ^{15}N-labelled azido-functionalized HEC, forming graft copolymers of HEC with different chain length and graft densities which were characterised using (^{13}C and ^{15}N) CP-MAS NMR and FT-IR spectroscopies. The antibacterial activities of HEC-g-P(IL)s were tested against *E. coli* and *S. aureus* and were comparable to ampicillin, a well-known antibiotic, demonstrating efficient activity of the graft copolymers against bacteria. Moreover, HEC-g-P(IL)s were slightly more effective against *E. coli* than *S. aureus*. A decrease in graft density of $P(IL)_{10}$ on the HEC backbone decreased the activity of the graft copolymers against both bacteria. These findings suggest that HEC-g-P(IL) could find applications as an antiseptic compound, for example in paint formulation.

Introduction

Synthetic, man-made polymers are produced from petroleum, a non-renewable resource. This will eventually result in decreased production of synthetic polymers with consequent societal problems because of their ubiquity in everyday life (packaging, furniture, containers, electronics, etc.). Polymers are also found in abundance in nature, in the form of biopolymers such as

cellulose, starch, proteins, amylose and chitin. In contrast to petroleum-based synthetic polymers, these polymers come from renewable sources. Cellulose is the most abundant biopolymer on Earth and is principally found in the cell walls of plants[1-3]. Cellulose, which is defined by the assembly of β-D-anhydroglucopyranose (AGU) units[4], presents interesting properties such as biocompatibility and high strength, however, its principal drawback is its insolubility in both organic and aqueous solvents, limiting considerably its use in industry[3, 5-7]. Chemical modification of the hydroxyl groups of cellulose overcomes this problem to some extent. In fact, hydroxyethyl cellulose (HEC) (Figure 1), where the hydroxyl groups have been modified with ethylene oxide, shows solubility in dimethyl sulfoxide and water due to the removal of the H-bonding networks of cellulose. Although the chemical modification of cellulose can improve considerably its physical properties, cellulose derivatives are still less competitive than synthetic polymers due to the latter's better solubility and easier production.

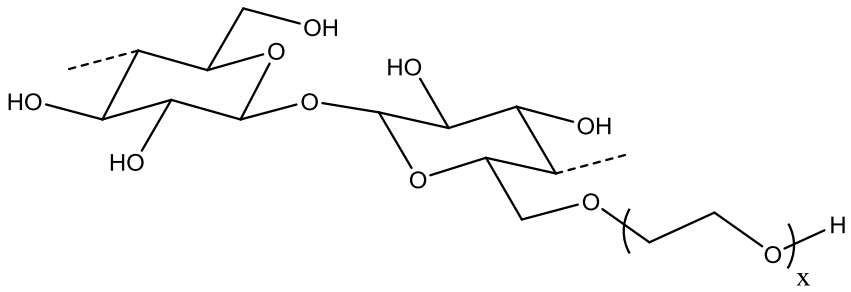

Figure 1. Chemical structure of HEC

Tashiro[8] and, more recently, Muñoz-Bonilla[9] reviewed advances in the preparation of antibacterial polymers which contain, for instance, quaternary ammonium salts, biguanide group and quaternary pyridinium, phosphonium or sulfonium salts. A new class of monomer, ionic

liquid monomers (IL), which include vinylimidazolium, methacryloyl and styrene-based ILs (Figure 2), have been developed recently and present promising properties such as high thermal stability, high ionic conductivity, low vapour pressure and bactericidal effects[10-12]. The antibacterial properties arise from the presence of the positive charge which disrupts the bacterial membrane leading to cell death.

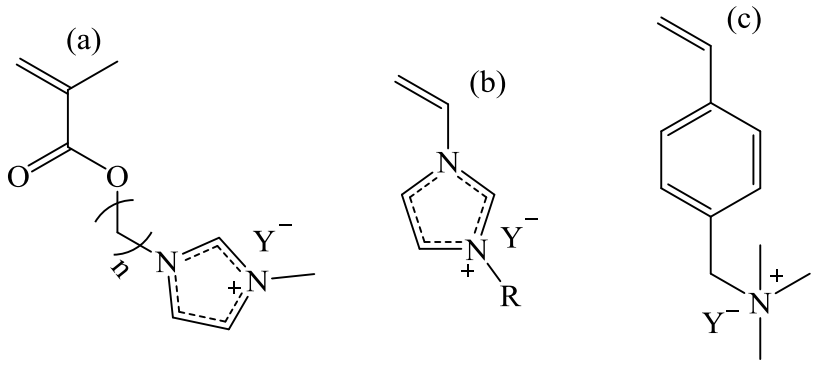

Figure 2. Structure of ionic liquid monomers (a) methacryloyl-, (b) vinyl-imidazolium- and (c) styrene- based IL

ILs have been polymerised successfully using conventional free radical polymerisation[13] and CRP techniques such as ATRP[14-16] and RAFT polymerisation[17, 18]. Regarding RAFT polymerisation, Mori *et al.*[17] used a xanthate-type chain transfer agent ('CTA') to polymerise vinylimidazolium salt-based ionic liquid (IL) monomers leading to a monomer conversion of up to 78% and dispersity ($Đ_M$) ranging from 1.2 to 1.4. Vijayakrishna *et al.*[18], however, used a dithiobenzoate CTA to polymerise methacryloyl-based IL monomers to a lower monomer conversion after a longer reaction time. The $Đ_M$ was not reported, however, the degree of

polymerisation was estimated using ^{1}H NMR spectroscopy and was in agreement with the monomer conversion.

Although HEC is used extensively as an emulsifier, stabiliser, thickener and cosmetic film-former in the formulation of personal care products and paints[19-21], it lacks antibacterial properties. Antibacterial compounds such as antibiotics are commonly mixed with cellulose to prevent the growth of microorganisms such as bacteria. In this work we sought to develop a hybrid HEC material possessing antibacterial properties via the introduction of cationic polymers, such as P(IL)s, as grafts on the HEC backbone. To prepare HEC-g-P(IL), our reported method[22] based on a "grafting to" approach, combining RAFT polymerisation and CuAAC, was used. An acryloyl-based IL monomer was chosen for the RAFT polymerisation because of the predicted higher reactivity of such a monomer compared to vinyl-imidazolium-based ILs. Here, we report the use of this method to form well-defined HEC graft copolymers containing different graft densities and graft lengths of P(IL), as well as their antibacterial behaviours and cytotoxicities against an immortalised lung alveolar cell line (A549).

2. EXPERIMENTAL

2.1. Materials

2-Hydroxyethyl cellulose (HEC) (M_w =90 kDa, MS =2.5), sodium azide (NaN_3), ^{15}N-labelled sodium azide ($Na^{15}N$), carbon tetrabromide, triphenylphosphine, propargyl bromide solution (80% wt. in toluene), potassium ethyl xanthogenate, 2,2′-azobis(2-methylpropionitrile) (AIBN), 11-bromo-1-undecanol, *p*-toluene sufonic acid, monomethyl ether hydroquinone (MEHQ),

acrylic acid, 1-methylimidazole, sodium L-ascorbate, copper (II) sulphate pentahydrate, N,N,N′,N′-tetramethylethylenediamine (TMEDA), dimethylformamide (DMF), pentane, cyclohexane, sodium hydroxide, magnesium sulfate, ampicillin sodium salt and Luria broth were purchased from Sigma Aldrich. Iso-sensitest broth was obtained from Oxoid^{TM}. Toluene, diethyl ether, acetone, tetrahydrofuran (THF) and dialysis tubing of 500-1,000 Da and 3,500 Da MWCO were supplied by Fisher Scientific. DMSO-d_6 was purchased from Apollo Scientific, and dialysis tubing of 50 kDa MWCO was supplied by Spectrumlabs. Both bacteria, *Escherichia coli* K-12 wild-type strain (W3110 / ATCC27325, F-, λ-, rpoS(Am), rph-1, Inv(rrnD-rrnE)) and *Staphylococcus aureus* (3R7089 strain Oxford / ATCC9144) were prepared in the laboratory. The A549 immortalized lung alveolar cell line was provided from the American tissue culture collection (ATCC). Dulbecco's Modified Eagle Medium (DMEM), Fetal Calf Serum (FCS) and Almar blue were purchased from Life Technologies Limited (UK).

2.2. Characterisations

Solution state NMR spectra were recorded using a Bruker Avance 400 spectrometer at 400.13 MHz (^{1}H) and 100.60 MHz (^{13}C). For solid state NMR spectroscopy, a Varian VNMRS spectrometer with a 9.4 T magnet was used and ^{13}C (100.562 MHz) and ^{15}N (40.527 MHz) experiments were run using the cross polarisation method. IR spectra were recorded on a Perkin-Elmer 1600 Series FT-IR spectrometer. Molecular weight and $Đ_M$ data were obtained using triple detection SEC on a Viscotek TDA 301 with refractive index, viscosity and light scattering detectors and 2 × 300 mL PL HFIPgel 9 μm columns. 1,1,1,3,3,3-Hexafluoropropan-2-ol with 25 mM of trifluoroacetic acid salt (NaTFAc) was used as the eluent at a flow rate of 0.8 mL/min

and at a constant temperature of 40 ºC. Experiments were performed by Smithers Rapra, Shawbury, UK.

2.3. Synthesis and characterisation

2.3.1. Preparation of N_3-HEC

The procedure followed that reported in the literature[23] (see Scheme 1). In a round-bottomed flask fitted with a condenser, 2-hydroxyethyl cellulose **1** (M_w =90,000 g/mol, MS =2.5, 2.5 g, 9.19×10^{-3} mol, 1 eq), sodium azide (3.8 g, 5.85×10^{-2} mol, 6 eq.) and ^{15}N-labelled sodium azide $Na^{15}N_3$ (0.1 g, 1.54×10^{-3} mol, 0.1 eq) were dissolved in DMF (100 mL). The mixture was heated at 80 °C for 1 h in order to dissolve HEC. The mixture was cooled to room temperature and carbon tetrabromide (14.3 g, 4.31×10^{-2} mol, 5 eq) was added. Triphenylphosphine (11.8 g, 4.50×10^{-2} mol, 5 eq) dissolved in DMF (12.5 mL) was added carefully to the HEC mixture. The reaction was then left for 24 h at room temperature under magnetic stirring. The product was precipitated by addition of toluene (500 mL) and collected by filtration. The solid was dissolved in DMF (50 mL) and re-precipitated using diethyl ether (500 mL). After being filtered, the solid was washed with acetone (100 mL) and dried under vacuum at 50 °C overnight. The product **2** was obtained as a light yellow solid in quantitative yield (3.1 g). The product was characterised using solid state (^{13}C and ^{15}N) CP-MAS NMR and FT-IR spectroscopies.

2.3.2. Preparation of the alkyne-terminated xanthate

The procedure followed that reported in the literature[24] (see Scheme S1). In a one-neck round-bottomed flask, propargyl bromide solution **3** (80% wt. in toluene, 1.02 g, 8.57×10^{-3} mol) and potassium ethyl xanthogenate **4** (1 g, 6.24×10^{-3} mol) were dissolved in THF (10 mL). The flask was covered with aluminium foil and the reaction was run overnight at room temperature. THF (100 mL) was added and the mixture was filtered to remove KOH. The excess solvent was evaporated and distilled water (10 mL) was added to the residues. The product was extracted with diethyl ether (3×30 mL). The diethyl ether was removed under vacuum and the final product **5** was purified via column chromatography using pentane as eluent and dried overnight under vacuum. The product was obtained as a pale yellow oil in a yield of 48% (0.48 g). ^{1}H NMR (400 MHz, DMSO-d_6): δ_H (ppm) 1.37 (t, J =7.0 Hz, 3H, C**H**$_3$-CH_2-O), 3.22 (t, J =2.6 Hz, 1H, C**H**≡C-), 3.97 (d, J =2.6 Hz, 2H, CH≡C-C**H**$_2$-), 4.65 (q, J =7.0 Hz, 2H, -C**H**$_2$-O); ^{13}C NMR (400 MHz, DMSO-d_6): δ_C (ppm) 13.5 (**C**H_3-CH_2-O-), 23.5 (-**C**H_2-S-), 70.6 (-**C**H_2-O-), 74.1 (**C**H≡C-), 78.6 (CH≡**C**-), 211.8 (-**C**=S).

2.3.3. Preparation of 1-(11-acryloyloxyundecyl)-3-methylimidazolium bromide

1-(11-acryloyloxyundecyl)-3-methylimidazolium bromide was prepared in a two-step procedure (Scheme 2) according to Harmand *et al.*[25]

First step: In a two-neck round-bottomed flask fitted with both a condenser and a dropping funnel, 11-bromo-1-undecanol **6** (2.5 g, 9.95×10^{-3} mol, 1 eq.), *p*-toluene sulfonic acid (0.2 g, 1.16×10^{-3} mol, 1 eq.) and MEHQ (0.02 g, 1.6×10^{-4} mol, 0.02 eq.) were dissolved in cyclohexane (27 mL) and the mixture was refluxed for 1 h. Acrylic acid **7** (0.8 mL, 1.16×10^{-2} mol, 1 eq.) was dissolved in cyclohexane (4 mL) and the solution was dropped into the reaction mixture using a

dropping funnel. The final mixture was refluxed overnight. Once cooled to room temperature, the organic solution of the product was washed with NaOH (10% w/w, 3×50 mL), dried over $MgSO_4$ and concentrated under vacuum. The product **8** was obtained in a yield of 88% (2.4 g). ^{1}H NMR (400 MHz, DMSO-d_6): δ_H (ppm) 1.30-1.80 (m, 18H, Br-CH_2-(C**H$_2$**)$_9$-), 3.52 (t, J =6.7 Hz, 2H, Br-C**H$_2$**-), 4.10 (t, J =6.7 Hz, 2H, -O-C**H$_2$**-), 5.94 (dd, J =10.3, 1.6 Hz, 1H, **H**CH=CH-), 6.17 (dd, J_{ac} =17.3, 10.3 Hz 1H, -C**H**-CH_2), 6.32 (dd, J =17.3, 1.6 Hz, 1H, HC**H**=CH-); ^{13}C NMR (100 MHz, DMSO-d_6): δ_C (ppm) 25.3-35.1 (9C, Br-CH_2-(**C**H_2)$_9$-), 40.4 (-**C**H_2-Br) 64.0 (-**C**H_2-O-), 128.4 (-CH=**C**H_2), 131.2 (-**C**H=CH_2), 165.4 (-**C**=O).

Second step: Bromoalkylacrylate **8** (2.4 g, 7.96×10^{-3} mol, 1 eq.), and 1-methylimidazole **9** (0.6 mL, 7.96×10^{-3}mol, 1eq.) were mixed and heated at 50 °C for 24 h. Once the mixture had cooled to room temperature, the product precipitated and was filtered. The product **10** was then washed with ether (3×50 mL) and dried under vacuum to obtain a white powder in a yield of 85% (2.6 g). ^{1}H NMR (400 MHz, DMSO-d_6): δ_H (ppm) 1.24-1.77 (m, 18H, -O-CH_2-(C**H$_2$**)$_9$-CH_2-), 3.86 (s, 3H, -N-C**H$_3$**), 4.08 (t, J =6.6 Hz, 2H, -O-C**H$_2$**-), 4.16 (t, J =7.2 Hz, 2H, CH_2-C**H$_2$**-N-), 5.95 (dd, J =10.3, 1.7 Hz, 1H, **H**CH=CH-), 6.15 (dd, J =20.3, 10.3 Hz, 1H, -C**H**-CH_2), 6.30 (dd, J =17.3, 1.6 Hz, 1H, HC**H**=CH-), 7.77 (dd, 2H, J =27.0, 0.97 Hz, -C**H**=C**H**-), 9.22 (s, 1H, -C**H**=N^+-); ^{13}C NMR (100 MHz, DMSO-d_6): δ_C (ppm) 25.3-35.1 (9C, Br-CH_2-(**C**H_2)$_9$-), 35.7 (N-**C**H_3), 48.7 (CH_2-**C**H_2-N-), 64.0 (-**C**H_2-O-), 122.2 (N-**C**H=CH-N) , 123.5 (N-CH=**C**H-N), 128.4 (-CH=**C**H_2), 131.2 (-**C**H=CH_2), 136.5 (-N-**C**H=N-), 165.4 (-**C**=O).

2.3.4. RAFT polymerisation of 1-(11-acryloyloxyundecyl)-3-methylimidazolium bromide

The following procedure was inspired by the work of Mori *et al.*[17] and Vijayakrishna *et al.*[18] (see Scheme 3). 1-(11-acryloyloxyundecyl)-3-methylimidazolium bromide (IL) **10** (10, 50 or 100 eq.), xanthate **5** (1 eq.) and AIBN (0.3 eq.) were dissolved in DMF (10 mL) and the mixture was purged with N_2 for 10 min. The flask was sealed and the reaction was heated at 70 °C for 17 h. The mixture was dialysed against water for 2 days using a dialysis tubing of MWCO of 500-1,000 g/mol for $P(IL)_{10}$ and 3,500 g/mol for $P(IL)_{50}$ and $P(IL)_{100}$. Subsequently the dialysed material was freeze-dried overnight and the polymer **11** was obtained as a sticky white solid in a yield of 70-80% (Table S1). The polymer was characterised using solution state NMR spectroscopy and SEC. NMR spectra were recorded in DMSO-d_6 and the M_n and $Đ_M$ values were determined using SEC with conventional calibration (PMMA standards).

2.3.5. CuAAC between N_3-HEC and alkyne-terminated poly(1-(11-acryloyloxyundecyl)-3-methylimidazolium bromide)

General procedure: in a round-bottomed flask fitted with a drying tube, N_3-HEC **2**, alkyne-terminated P(IL) **11**, sodium L-ascorbate (2 eq.), copper (II) sulfate pentahydrate (1 eq.) and N,N,N′,N′-tetramethylethylenediamine (1 eq.) were dissolved in DMF (20 mL). The flask was heated at 30 °C for 24 h. The mixture was cooled to room temperature and dialyzed for 3 days using a 50 kDa MWCO membrane against Milli-Q water (18.2 Mega Ohm). HEC-g-P(IL) **12** was further lyophilized and obtained in a yield ranging from 64-100% (Table S2). The graft copolymers were characterized using solid state (^{13}C and ^{15}N) CP-MAS NMR and FT-IR spectroscopies.

2.4. Biological study

2.4.1. Anti-bacterial testing

The bacteriological effects of the HEC_m-g-$P(IL)_n$s **18** containing P(IL) with different chain lengths (n= 10, 50 and 100; m =1) and different graft densities (m =1, 0.3 and 0.17; n =10) were investigated using an *Escherichia coli* K-12 wild-type strain (W3110)[26], and *Staphylococcus aureus* (3R7089 strain Oxford)[27] selected as representative Gram-negative and Gram-positive species, respectively.

Bacterial growth inhibition assay on agar plates

HEC_m-g-$P(IL)_n$s were dissolved in Oxoid™ iso-sensitest broth at a concentration of 10 mg/mL and 6 sequential 2-fold dilutions were prepared in the same medium. 10 µL of each dilution was spotted onto a Luria-Bertani (LB) agar plate containing bacteria in a 0.6% soft agar overlay (5 mL) and the plates incubated overnight at 30 °C. Samples were analysed in triplicate and a zone of growth inhibition was observed due to the presence of the HEC_m-g-$P(IL)_n$s.

Determination of minimum inhibitory concentration (MIC)

MIC determination followed the protocol described by Andrews[28]. 10 mg/mL dilution of HEC_m-g-$P(IL)_n$s in iso-sensitest broth were prepared and 11 sequential 2-fold dilutions were made using the medium as diluent. The inoculum was prepared from a single bacterial colony grown on LB agar plates and inoculation of 5 mL of iso-sensitest broth followed by incubation overnight at 37 °C. 20-50 µL of overnight culture was inoculated into 1 mL of iso-sensitest broth

and incubated at 37 °C with aeration until an inoculum density of approximatively 10^4 cfu/spot was reached as determined by an optical density A_{650nm} of 0.07, equivalent to a 0.5 MacFarland standard (240 µM $BaCl_2$ in 0.18 M $H_2SO_{4\ aq.}$). This inoculum was diluted 10-fold in iso-sensitest broth for use in MIC determination.

In a 96-well microtiter plate, 50 µL of each dilution of HEC_m-g-$P(IL)_n$ was mixed with 50 µL of inoculum for each dilution. Ampicillin was diluted in a similar manner as HEC_m-g-$P(IL)_n$s and was used as a positive antibacterial control. The plate was incubated at 37 °C overnight with shaking and the optical density A_{650nm} of each well was recorded using a Biotek Synergy HT Multi-Mode Microplate Reader. Samples were analysed in triplicate.

2.4.2. Measurement of cytotoxicity

A549, an immortalized lung alveolar cell line[29], was cultured in DMEM supplemented with 10% FCS. Approximately 5×10^3 cells in a volume of 100 µL per well were used to seed a 96-well plate. Cells were allowed to grow in a humidified incubator with an atmosphere of 5% CO_2 at 37 °C until 70% confluence was achieved. HEC_m-g-$P(IL)_n$s to be tested were dissolved in culture medium to a concentration of 1 mg/mL and 100 µL was added to each well of the first column of wells to give a final concentration of 500 µg/mL. Subsequently 2-fold serial dilutions were performed from columns 1-11 with the final column being left as a negative control. After further incubation the effect of the treatment was determined by a cell viability assay using Almar Blue[30] (GIBCO) that was analysed on a fluorescent plate reader (BioTek, FL500) using the GEN5 software package. Samples were analysed four times to ensure the reliability of the results. The fluorescence was read using a fluorescence excitation and emission wavelengths of

540–570 nm (peak excitation is 570 nm) and 580–610 nm (peak emission is 585 nm) respectively. The evolution of the fluorescence intensity as a function of the concentration of HEC-g-P(IL) permitted the graphical determination of LD_{50}.

3. RESULTS AND DISCUSSION

3.1. Graft copolymers of HEC

3.1.1. Azide functionalized hydroxyethyl cellulose: N_3-HEC

N_3-HEC **2** was prepared from HEC **1** using a one-step procedure[23] (Scheme 1). In order to aid the detection of nitrogen by ^{15}N NMR spectroscopy, sodium azide was doped with $Na^{15}N_3$. The characterisation of the partially labelled N_3-HEC has already been described in our previous work[22], where the efficiency of a method combining click reaction and RAFT polymerisation to prepare graft copolymers of HEC was demonstrated, and resulted in the full functionalization of the primary alcohols of HEC with NaN_3. For simplicity, Scheme 1 only shows substitution at the C6 position, however, substitution at positions C2 and C3 cannot be ruled out.

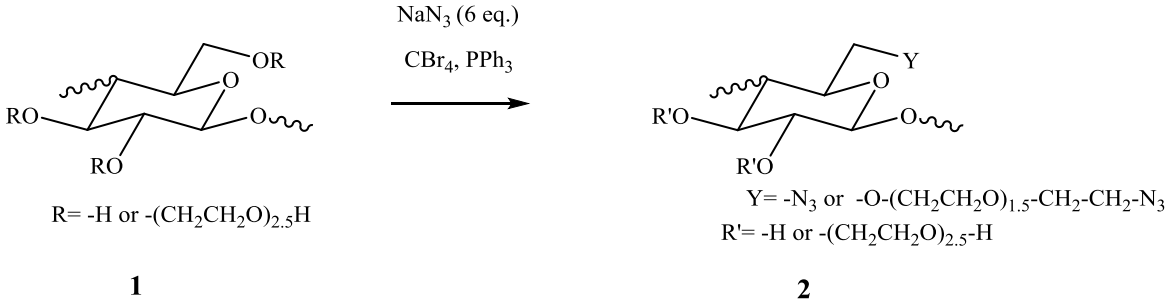

Scheme 1. Synthesis of partially ^{15}N-labelled N_3-HEC **2**.

3.1.2. Poly(1-(11-acryloyloxyundecyl)-3-methylimidazolium bromide)

1-(11-acryloyloxyundecyl)-3-methylimidazolium bromide **10** was synthesised in 75% overall yield following the two-step procedure of Harmand *et al.*[25], as shown in Scheme 2. It was then polymerised by RAFT polymerisation using xanthate **5** as chain transfer agent (Scheme 3). A xanthate CTA was chosen because the imidazolium ring could potentially reduce the reactivity of the acrylate functionality.

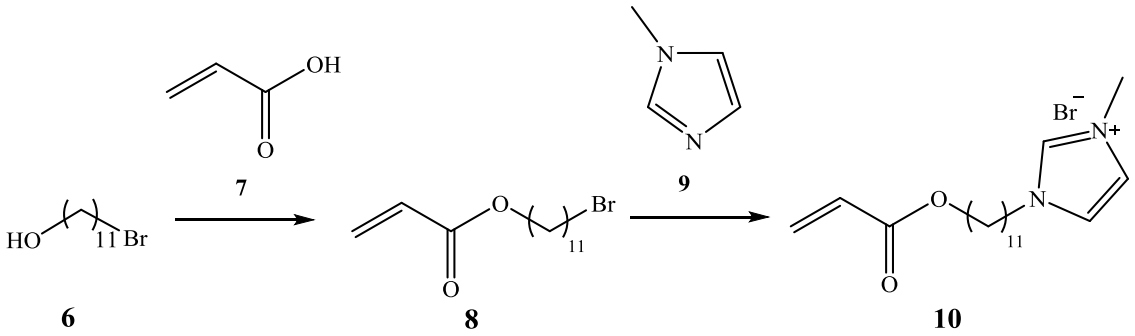

Scheme 2. Preparation of 1-(11-acryloyloxyundecyl)-3-methylimidazolium bromide **10**.

The polymerisation of IL **10** (Scheme 3) was inspired by the work of Mori *et al.*[17] and Vijayakrishna *et al.*[18]. RAFT polymerisation was performed at 70 °C in DMF using a ratio of xanthate to initiator (AIBN) of 1:0.3 which led to a good comprise between monomer conversion and dispersity. Different degrees of polymerisation (10, 50 and 100) were targeted in order to produce graft copolymers of HEC with different chain lengths. After 17 h of polymerisation, the monomer conversion determined using ^{1}H NMR spectroscopy was found to be approximatively 70-80% (Table S1). Subsequently, the P(IL)s **11** were characterised by NMR spectroscopy and SEC.

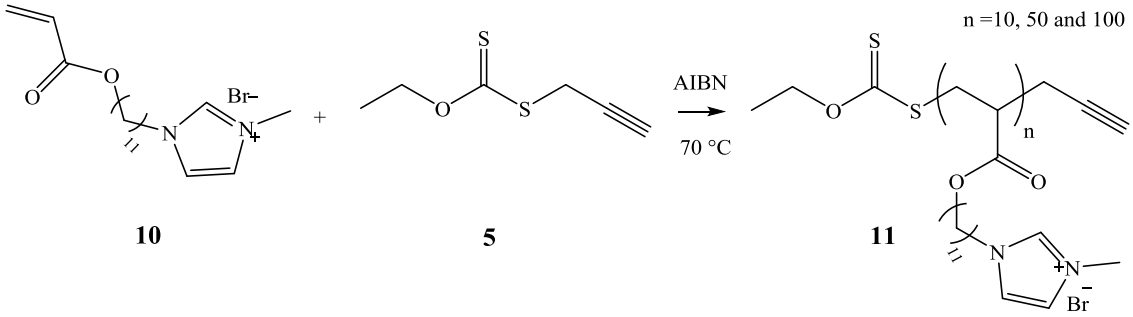

Scheme 3. RAFT polymerisation of 1-(11-acryloyloxyundecyl)-3-methylimidazolium bromide (IL) **10**.

In the ^{1}H NMR spectrum of P(IL)$_{100}$ (Figure 3), signals δ_H ~1.2-1.8 ppm are assigned to the -C**H**$_2$ protons along the side chain and the backbone of P(IL). The signal δ_H ~2.2 ppm is assigned to the methine group of the backbone and the signal δ_H ~3.9 ppm is assigned to the -C**H**$_3$ group which is the substituent group of the ring. The signal δ_H ~4 ppm is assigned to -C**H**$_2$- next to the imidazolium ring and the signal δ_H ~4.2 ppm is assigned to the protons –C**H**$_2$ next to the acrylate group. The signal δ_H~ 7.7-7.8 and 9.4 ppm are assigned to the protons of the imidazolium ring. The signals of the end groups were not found, perhaps because they are hidden by the signals of P(IL) because they are too weak. The absence of peaks in the range δ_H ~6.0-6.5 ppm in the ^{1}H NMR spectrum confirms that dialysis was successful in removing any residual monomer, and thus the purity of the polymer can be estimated at > 99%. The spectra of the P(IL)$_{50}$ and P(IL)$_{10}$ did not show any new signals, thus, the estimation of the chain length from end groups analysed by NMR spectroscopy was not feasible.

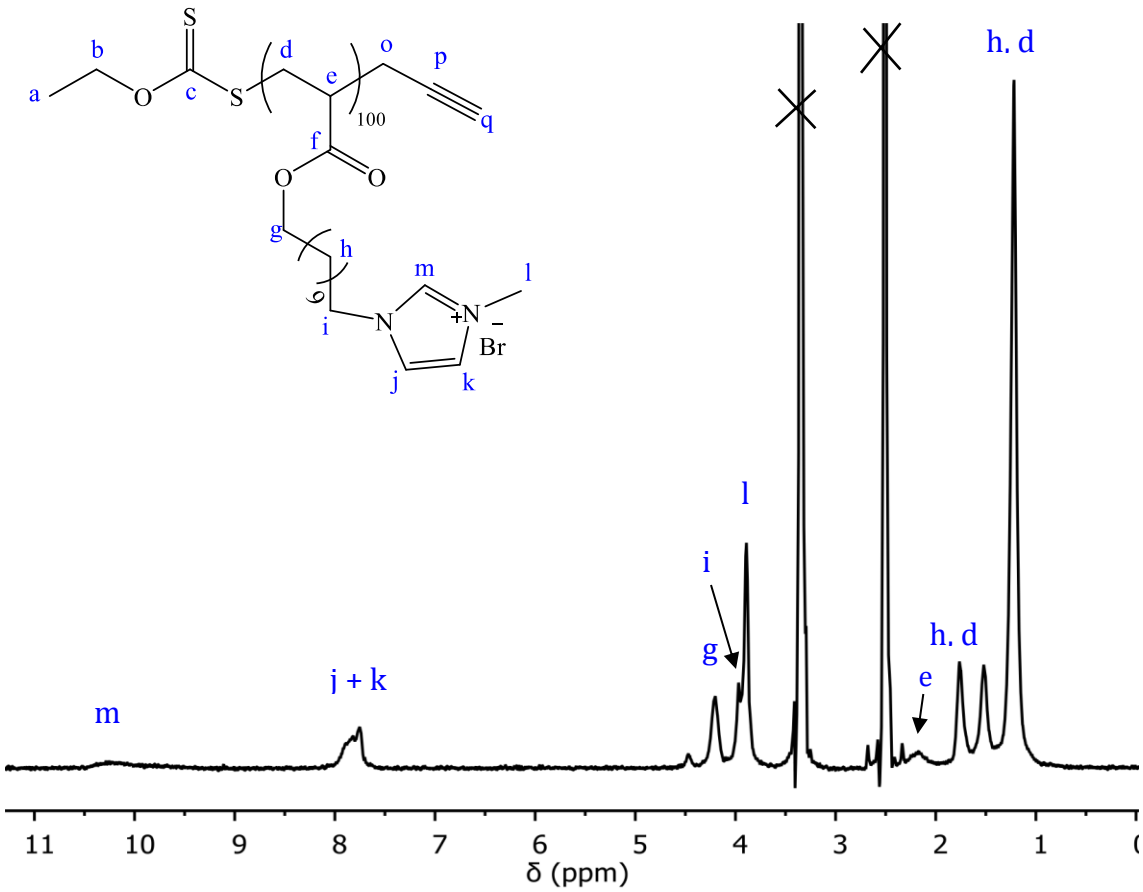

Figure 3. Solution state ^{1}H NMR spectrum of poly(1-(11-acryloyloxyundecyl)-3-methylimidazolium bromide) ($DP_{targeted}$=100)

The molecular weight and dispersity of P(IL) were determined using SEC. The SEC trace for $P(IL)_{100}$ is displayed in Figure 4. Conventional calibration with PMMA standards was used to determine M_n and was found to be 26,600 g/mol. This is in good agreement with the predicted M_n at 71% monomer conversion (27,600 g/mol). A $Đ_M$ of 1.5 was measured, indicating some control of the polymerisation. A value of $Đ_M$ below 1.2 is widely accepted to indicate full control of the polymerisation, while a value between 1.2 to 1.5 indicates some control of the polymerisation. A value greater than 1.5 means the loss of control resulting in a broader

molecular weight distribution. Typically, polymers produced *via* conventional free radical polymerisation have a $Đ_M$ value higher than 1.5. The dispersity value of 1.5 for $P(IL)_{100}$ was borderline for a polymer which was prepared from a reversible deactivation radical polymerization (RDRP) process. Regarding P(IL)s with shorter chain lengths (DP = 10 and 50), $Đ_M$ values are expected to be similar or slightly higher because the lower DP accentuates differences in chain lengths.

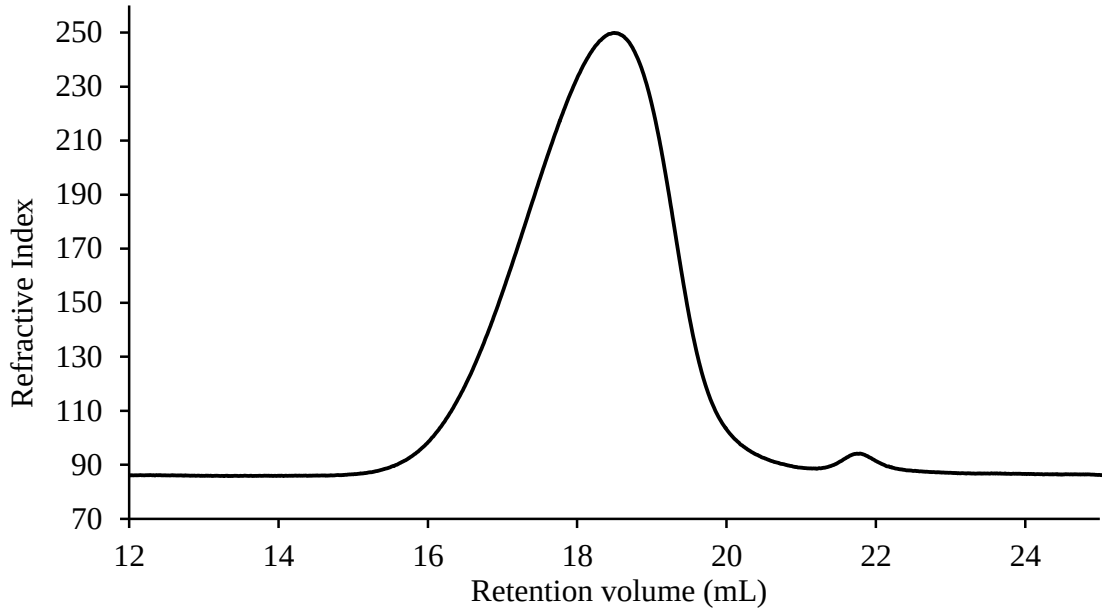

Figure 4. SEC trace of $P(IL)_{100}$.

3.1.3. Graft copolymers HEC-g-poly(1-(11-acryloyloxyundecyl)-3-methylimidazolium bromide): HEC-g-P(IL)s

Ionic liquid polymers $P(IL)_n$ **11** of different chain lengths (n =10, 50 or 100) were coupled to each AGU unit of N_3-HEC **2** and this resulted in the preparation of graft copolymers HEC-g-$P(IL)_n$s **12** (Scheme 4) where the grafts were composed of 10, 50 or 100 repeat units of ionic liquid monomer. These fully substituted HEC graft copolymers thus have a graft density of 1. Additionally, HEC_m-g-$P(IL)_{10}$s were prepared with different graft densities (m =0.3 and 0.17) via the coupling of one $P(IL)_{10}$ chain per 3 and 6 AGU units of N_3-HEC respectively. In order to remove the homopolymer $P(IL)_n$, the reaction mixture was dialysed against water using a dialysis tubing of a MWCO of 50,000 g/mol ensuring the recovery of only HEC_m-g-$P(IL)_n$s. The graft copolymers were characterised using solid state (^{13}C and ^{15}N) CP-MAS NMR and FT-IR spectroscopies. Their solubility permits characterisation by solution state NMR spectroscopy, however the resulting spectra do not show the presence of HEC and thus evidence of the coupling could not be demonstrated. The chain length (defined by "n") of P(IL) did not influence the detection of the HEC backbone by solid state NMR spectroscopy, however, decreasing the graft density (defined by "m") allowed the presence of HEC to be confirmed. The characterisation of HEC_m-g-$P(IL)_{10}$s (m =1, 0.3 and 0.17) only are reported here.

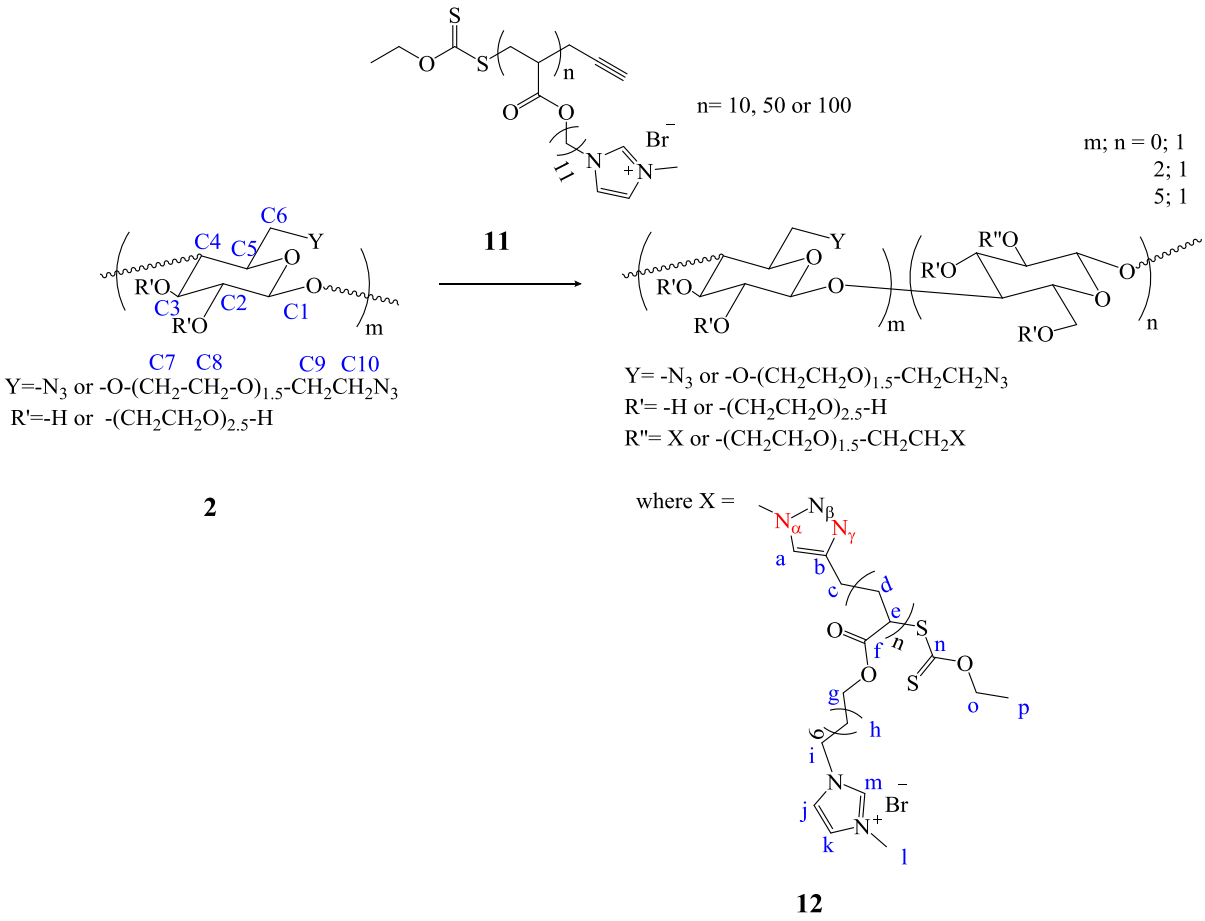

Scheme 4. CuAAC between alkyne-ended P(IL)$_n$ and partially ^{15}N-labelled N$_3$-HEC

FT-IR spectra of N$_3$-HEC, P(IL)$_{10}$ and HEC$_m$-g-P(IL)$_{10}$s are displayed in Figure 5. The total loss of the azide signal at 2136 cm^{-1} in the spectrum of HEC$_1$-g-P(IL)$_{10}$ (Figure 5d) indicates the complete consumption of the azide group of N$_3$-HEC (Figure 5a) due to the formation of the triazole with the alkyne-terminated P(IL)$_{10}$. This is crucial evidence of the grafting because, otherwise, the IR spectrum of HEC$_1$-g-P(IL)$_{10}$ is the same as that of P(IL)$_{10}$ (Figure 5e), and no absorption bands of HEC were detected because they are probably hidden by those of P(IL)$_{10}$. On decreasing the graft density (Figure 5b & c), the azide signal at 2136 cm^{-1} was still detected,

however a decrease of its relative intensity was observed compared to the IR spectrum of N_3-HEC (Figure 5a) indicating partial consumption of the azide. In fact, increasing the graft density produces a decrease of the relative intensity of the azide signal (Figure 5c vs. 5b). Except for this signal, the others are characteristic of the presence of $P(IL)_{10}$. The bands at 3400 cm^{-1} are assigned to -OH groups, at ~3142 cm^{-1} to the -CH groups of the ring, at 2856-2926 cm^{-1} to the alkyl -CH groups, at 1734 cm^{-1} to the carbonyl group, at 1676 cm^{-1} to the -C=C- and -C=N- groups, at 1576 cm^{-1} to the -C-C- and -C-N- groups, at 1468 cm^{-1} to the -CH alkyl groups and at ~1170 cm^{-1} to the alkyl -CH groups.

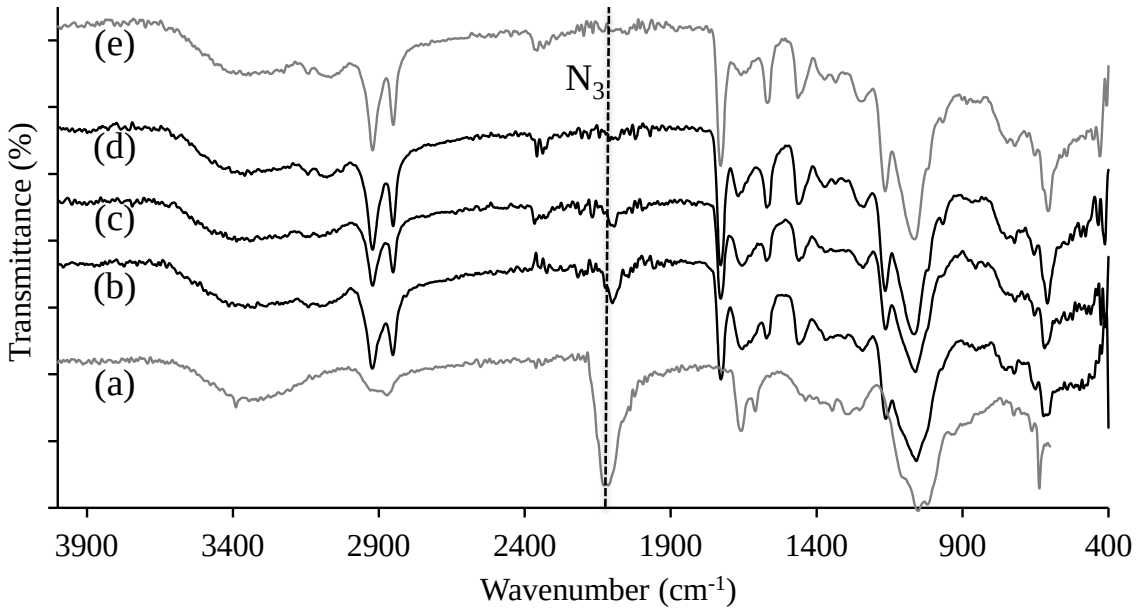

Figure 5. FT-IR spectrum of: (a) N_3-HEC; (b) $HEC_{0.17}$-g-$P(IL)_{10}$; (c) $HEC_{0.3}$-g-$P(IL)_{10}$; (d) HEC_1-g-$P(IL)_{10}$; and (e) $P(IL)_{10}$.

The solid state ^{13}C CP-MAS NMR spectrum of HEC_1-g-$P(IL)_{10}$ (Figure 6c) shows only signals of the $P(IL)_{10}$ grafts. The signal $\boldsymbol{\delta}_C$ ~174.4 ppm is assigned to the carbonyl group, $\boldsymbol{\delta}_C$ ~139.5 and ~123.6 ppm are assigned to the alkyl -**C**H groups of the ring, $\boldsymbol{\delta}_C$ ~64.9 ppm to the -**C**H_2-O group, $\boldsymbol{\delta}_C$ ~49.1 ppm to the -**C**H_2-N group, $\boldsymbol{\delta}_C$ ~41.4 ppm to the methine group and the signals $\boldsymbol{\delta}_C$ ~36.0-30.6 ppm to the methylene and methyl groups. The absence of signals for the HEC backbone was expected because of the relatively high molecular weight of the $P(IL)_{10}$ grafts. In our previous work[22], coupling of polymers with N_3-HEC was demonstrated more easily because of the low molecular weight of the grafted chains (PVP_{10} or $PNIPAAM_{10}$) which did not exceeded 1,000 g/mol. The signals assigned to the HEC backbone, which were relatively weak compared to those of the grafts, were detected in the solid state ^{13}C NMR spectra[22], however, we suspected that an increase in the molecular weight of the grafts would result in the disappearance of the signals of HEC. This is what we observed with $P(IL)_{10}$ grafts, which have a molecular weight of approximatively 4,000 g/mol. However, a decrease of the graft density permitted the detection of the HEC backbone. In fact, signals assigned to HEC were clearly detected in the spectrum of $HEC_{0.17}$-g-$P(IL)_{10}$ (Figure 6a) which possesses the lowest graft density of $P(IL)_{10}$. The signal $\boldsymbol{\delta}_C$ ~103.6 ppm is assigned to the carbon at the C1 position, ~82.6 ppm to carbon at the C4 position, ~74.9 ppm to the set of carbons at C2, C3 and C5 positions, ~71.2 ppm to the set of carbons at C6, C7, C8 and C9 positions and ~51.1 ppm to the carbon at C10 position. These signals assigned to the HEC backbone were still detected in the spectrum of $HEC_{0.3}$-g-$P(IL)_{10}$ (Figure 6b) but their relative intensities are lower due to the increase of the graft density of $P(IL)_{10}$ compared to those in the spectrum of $HEC_{0.17}$-g-$P(IL)_{10}$.

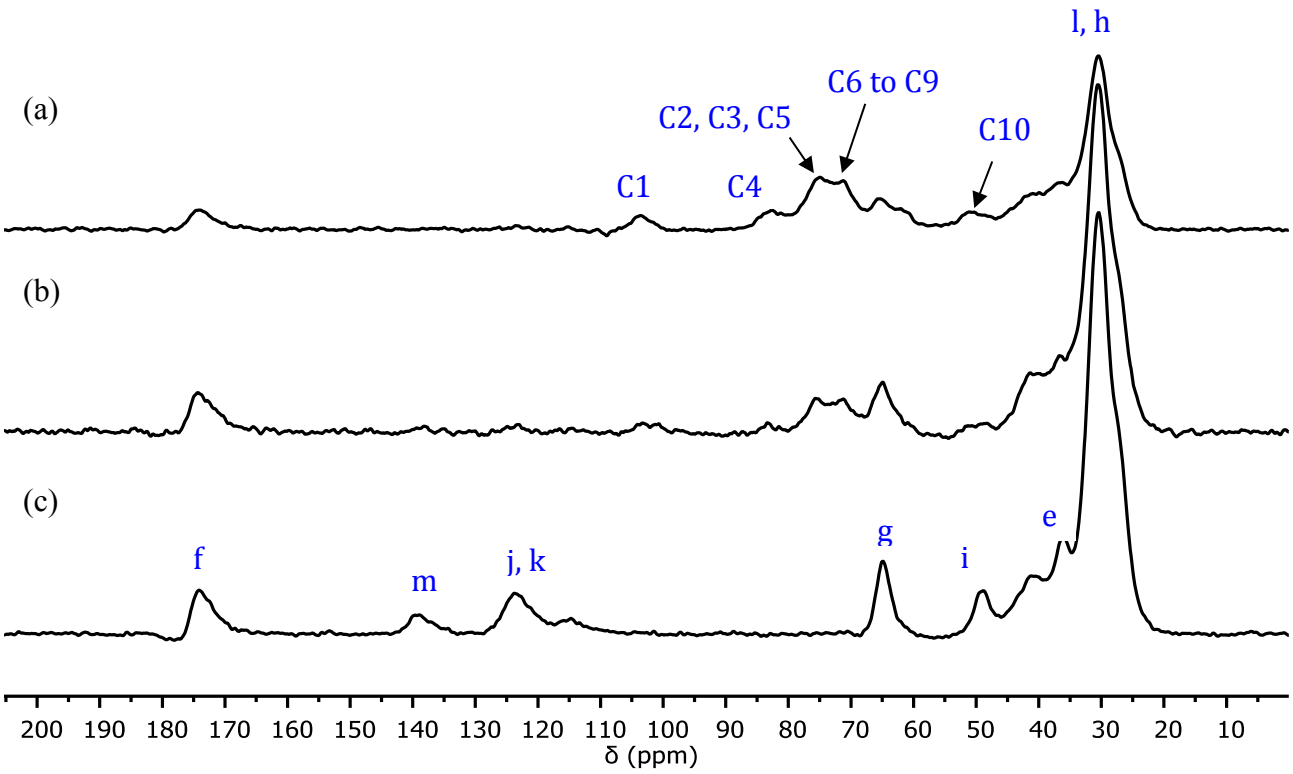

Figure 6. Solid state ^{13}C CP-MAS NMR spectra of HEC_m-g-$P(IL)_{10}$: (a) $HEC_{0.17}$-g-$P(IL)_{10}$; (b) $HEC_{0.3}$-g-$P(IL)_{10}$; (c) HEC_1-g-$P(IL)_{10}$.

The solid state ^{15}N spectra of HEC_1-g-$P(IL)_n$ with n =10, 50 and 100 were all identical, thus only the spectrum of HEC_1-g-$P(IL)_{10}$ is reported here (Figure 7b) with the spectrum of N_3-HEC (Figure 7a) used as a reference. The spectrum of N_3-HEC showed two signals $\boldsymbol{\delta}_N$ ~ –310 ppm and ~ –170 ppm which are assigned to N_α and N_γ respectively (Scheme 4)[31, 32]. The differences in intensity can be explained by the differences in their proton environment. N_α is next to a methylene group resulting in a higher intensity of its signal compared to that of N_γ because nitrogen is detected through the excitation of the protons. From our previous investigation[22], only the N_α signal remained in the ^{15}N CP-MAS NMR spectrum after cycloaddition of N_3-HEC with

alkyne-terminated synthetic polymers, however, the signal was shifted from ~ –310 ppm to ~ –134 ppm, providing evidence of the success of the "click" reaction. Here, the spectrum of HEC_1-g-$P(IL)_{10}$ showed two signals $\boldsymbol{\delta}_N$ ~ –208.0 and ~ –194.3 ppm which are assigned to the imidazolium ring, based on the literature[33]. More precisely, the former is assigned to the -N-CH_3 group and the latter to the N-CH_2- group. The absence of the signal $\boldsymbol{\delta}_N$ ~ –134 ppm, assigned to N_α after the cycloaddition, is most likely caused by the high molecular weight of the $P(IL)_{10}$ grafts which decreases the relative intensity of the N_α signal. Decreasing the graft density of $P(IL)_{10}$ resulted in the loss of signals assigned to the nitrogen atoms nitrogen present in the grafts, however, the signals assigned to the triazole and azide were also absent. In fact, a decrease of the graft density did not change the ratio of N_α (after cycloaddition) to $P(IL)_{10}$, and this is why N_α remains undetectable. N_α and N_γ (before cycloaddition) were also not detected upon decreasing the graft density because their concentration is too low compared to the rest of the sample.

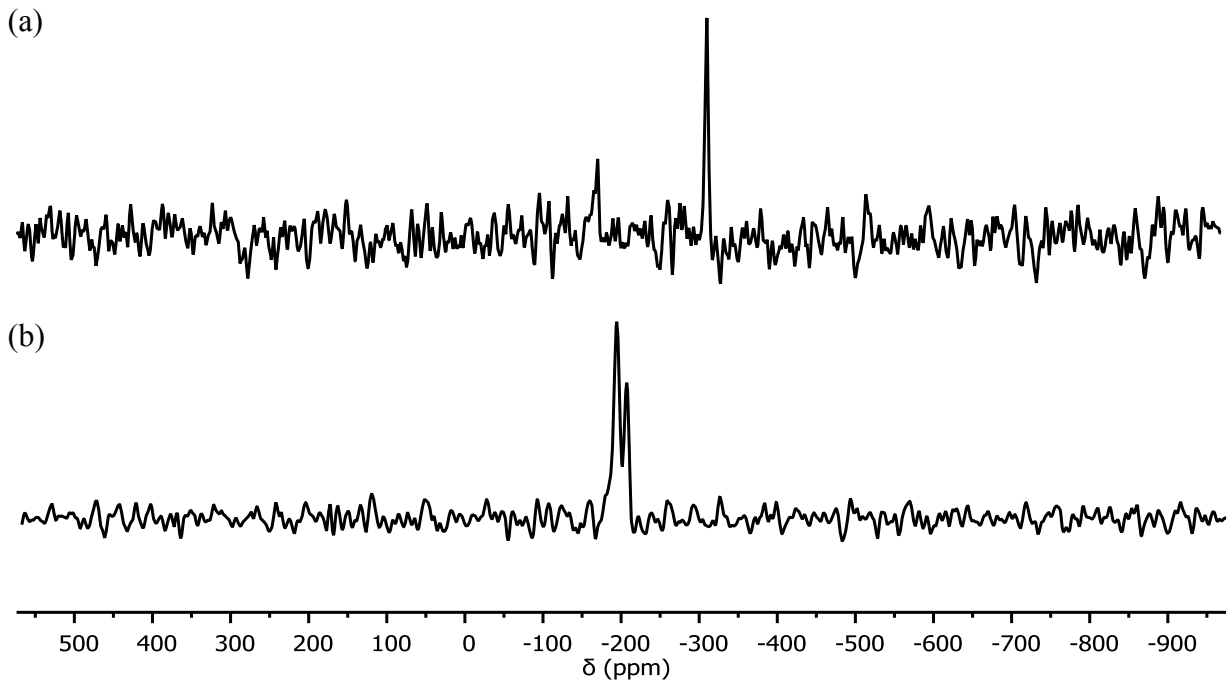

Figure 7. Solid state ^{15}N CP-MAS spectra: (a) N_3-HEC; (b) HEC_1-g-$P(IL)_{10}$

To summarise, the characterisation of the graft copolymers demonstrated the presence of P(IL) grafts by NMR and FT-IR spectroscopies, however, detection of the HEC backbone was more challenging due to the high molecular weight of the IL monomer. When the graft density of $P(IL)_{10}$ was decreased, the HEC backbone was detected by ^{13}C CP-MAS NMR spectroscopy indicating the presence of HEC in the product. The use of ^{15}N CP-MAS NMR spectroscopy did not demonstrate the formation of the triazole, most probably because of the relatively low level of enrichment over the 0.4% background. However, evidence of coupling between P(IL)s and N_3-HEC came from the disappearance of the azide band at 2100 cm^{-1} in the FT-IR spectrum of the graft copolymers. Furthermore, a quantitative yield for each coupling reaction (Table S2) strongly implies coupling of the azide in N_3-HEC, resulting in the preparation of HEC based

P(IL) graft copolymers. The final graft copolymers were purified by extensive dialysis using a high molecular weight cut off membrane (50,000 g/mol) so it can reasonably be expected that any uncoupled P(IL) chains were removed.

3.2. Biological activities of HEC-g-P(IL)s

The successful preparation of HEC-g-P(IL)s **12** permitted the study of their effects on bacteria and on an immortalized lung alveolar cell line (A549) to investigate potential applications. Furthermore, the influence of the chain length and the graft density of P(IL) on biological activity were investigated.

3.2.1. Antibacterial effects

Two tests were performed to evaluate the bacteriological effects of the HEC-g-P(IL)s. The first was a qualitative test to visualise any effects on growth inhibition, whereas the second was a quantitative test permitting a determination of the minimum inhibition concentration (MIC) which is the lowest concentration of a compound which inhibits bacterial growth. *E. coli* (Gram-negative) and *S. aureus* (Gram-positive) were chosen as representative bacteria.

Solutions of each HEC_m-g-$P(IL)_n$ were prepared using iso-sensitest broth and series of 11 x 2-fold dilutions were prepared resulting in concentrations ranging from 10 mg/mL to 2 µg/mL. In the first test, which shall be referred to as the zone inhibition assay, 10 µL of each solution of the first 6 dilutions were spotted onto an agar plate containing an overlay of *E. coli* or *S. aureus*

bacteria. The plates were incubated overnight to allow the lawn of bacteria to grow (Figure 8). To determine the MIC (2nd test), 50 μL of each graft copolymer solution was pipetted into a 96-well plate containing 50 μL of bacteria solution (both in iso-sensitest broth). The 96-well plate was incubated overnight and the optical density (OD) at A_{650nm} was determined in each well to monitor bacterial growth (Figure 9). A 10 mg/mL dilution series of ampicillin was used as a positive control.

For *E. coli,* growth inhibition (Figure 8a) was obtained from solutions of $P(IL)_n$-g-HEC_1s with concentrations ranging from 10 to 1.75 mg/mL, independent of the graft chain length (n = 10, 50 and 100). At 0.875 mg/mL HEC_1-g-$P(IL)_n$ (with n = 100, 50 and 10) concentration, inhibition was not observed indicating the loss of antibacterial effect at this concentration. At 1.75 mg/mL, the size of the zones were similar independent of the length of P(IL) grafts, indicating there was no major influence of the chain length on antibacterial properties. However, the graft density of $P(IL)_{10}$ on HEC affected to a slight extent the inhibitory effect. The inhibitory effect of the graft copolymers with lower graft densities (m =0.3 and 0.17) was shown at higher concentration than HEC_1-g-$P(IL)_{10}$. At a 1.75 mg/mL HEC_m-g-$P(IL)_{10}$ (with m =0.3 and 0.17) concentration, inhibition zones were not observed indicating the lack of an inhibitory effect. Furthermore, the size of the inhibition zones for $HEC_{0.3}$-g-$P(IL)_{10}$ and $HEC_{0.17}$-g-$P(IL)_{10}$ were similar at a concentration of 2.5 mg/mL, demonstrating a limited influence of the graft density on inhibition at these densities. However, HEC_1-g-$P(IL)_n$ (n =10, 50 and 100) also have a higher inhibitory effect compared to those of lower graft density.

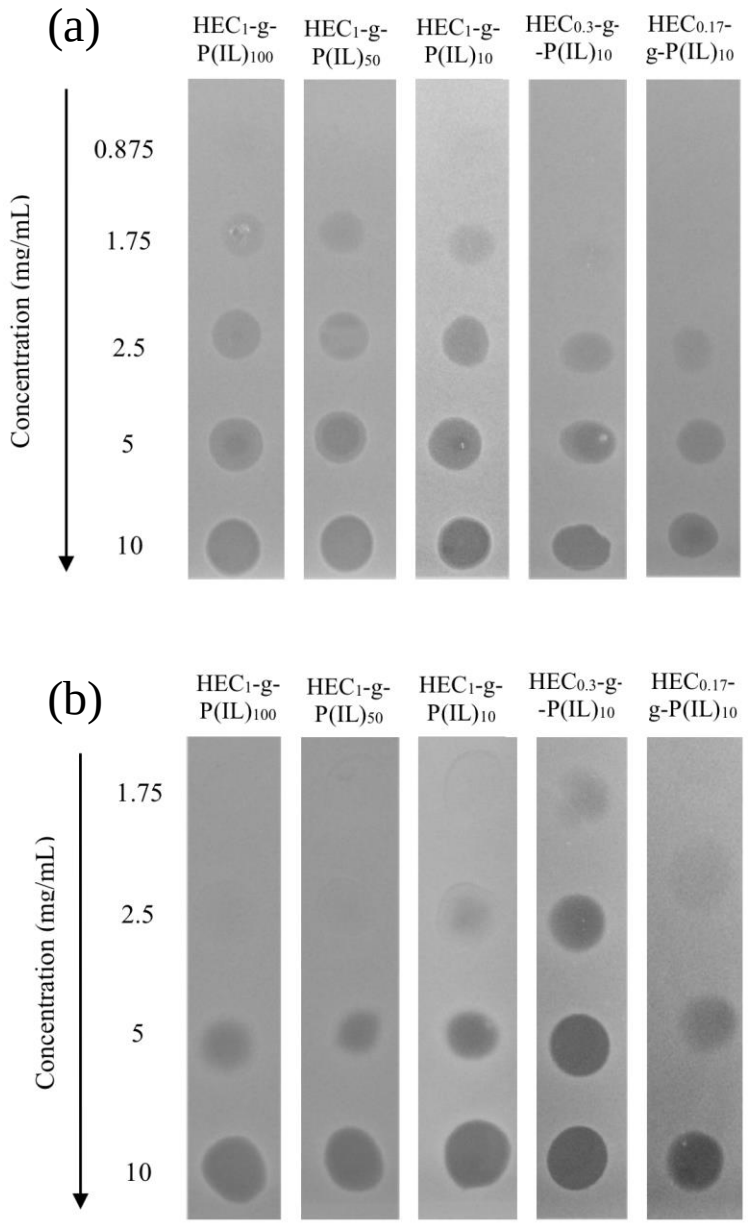

Figure 8. Results of the zone inhibition assays for the graft copolymers HEC-g-P(IL)s against (a) *E. coli* (b) *S. aureus*.

For *S. aureus*, zones of growth inhibition were observed at 10 and 5 mg/mL concentrations for each graft copolymers (Figure 8b), however, at 2.5 mg/mL concentration, HEC_1-g-$P(IL)_{10}$ and $HEC_{0.3}$-g-$P(IL)_{10}$ still showed a slight growth inhibition, whereas HEC_1-g-$P(IL)_{50}$, HEC_1-g-$P(IL)_{100}$ and $HEC_{0.17}$-g-$P(IL)_{10}$ did not. Samples with longer grafts of IL (50 and 100) or a decreased graft density ($HEC_{0.17}$-g-$P(IL)_{10}$) had a similar effect on the growth of *S. aureus* bacteria.

In order to corroborate these observations, MICs for each bacterial strain with the different graft copolymers were determined. Regarding *E. coli*, the graft copolymers HEC_1-g-$P(IL)_n$s (n =10, 50 and 100) and HEC_m-g-$P(IL)_{10}$s (m =0.3 and 0.17) gave MIC values of 10 and 19 μg/mL respectively (Figure 9a). Furthermore, a MIC value of 39 μg/mL was measured for ampicillin, higher than that determined for HEC-g-P(IL)s demonstrating a stronger inhibitory effect of the graft copolymers against Gram-negative bacteria. For *S. aureus*, MIC values for HEC_1-g-$P(IL)_{10}$ and $HEC_{0.3}$-g-$P(IL)_{10}$ were estimated to be 19 μg/mL whereas a MIC value of 39 μg/mL was determined for HEC_1-g-$P(IL)_n$ (n =50 and 100) and $HEC_{0.17}$-g-$P(IL)_{10}$ (Figure 9b). The MICs of HEC_1-g-$P(IL)_n$ (n =100 and 50) and $HEC_{0.17}$-g-$P(IL)_{10}$ were similar to that of ampicillin, however, the MICs of HEC_m-g-$P(IL)_{10}$s (m =1 and 0.3) were lower, suggesting a potentially stronger efficacy of these graft copolymers against Gram-positive bacteria compared to a well-known antibiotic.

To summarise, growth inhibition effects of the graft copolymers on both Gram-positive and Gram-negative bacteria were observed. The magnitude of the effects were comparable to those produced by ampicillin, a commonly used antibiotic. The cationic charge of the imidazolium ring is likely to be responsible for this effect[8]. Surprisingly, the chain length of the grafts, which determines the number of charges, did not significantly influence the antibacterial properties of

HEC-g-P(IL)s against *E. coli*.. However, a decreased graft density of $P(IL)_{10}$ on the HEC backbone increased the MIC, suggesting a reduction of the antibacterial effect. This suggests that the antibacterial activity results from the presence of the cationic charge at the outer surface and does not rely on the number of charges in the graft copolymer. A decreased chain length therefore improved the antibacterial effect whereas a decreased graft density reduced the antibacterial action. The antibacterial activity was slightly stronger using graft copolymers with shorter chains and one plausible explanation could be the accessibility of the cationic charges which disrupt the cell wall envelope of the bacteria resulting in its death. Graft copolymers with long grafts could adopt different conformations limiting the accessibility of the cationic charge for the bacteria and thus the antibacterial power. The MIC values against *S. aureus* were higher than against *E. coli* suggesting that the antibacterial activity of the graft copolymers is slightly stronger against *E. coli* than against *S. aureus*; the improved resistance of *S. aureus* over *E. coli* was also evident in zone inhibition assay (Figure 8). The mechanism of the inhibitory effect most likely resides in the interaction between the cationic charge and the bacterial membrane. Gram-positive and Gram-negative bacteria cell envelopes differ significantly in terms of structure, permeability and density of charge. The *S. aureus* phospholipid bilayer is protected by a thick outer layer of peptidoglycan further stabilised by teichoic acids[34] which may partially restrict direct contact of graft copolymers with the bacterial membrane. In order to destabilise the *S. aureus* membrane the concentration of HEC-g-$P(IL)_n$ had to be higher compared to that for *E. coli* where the outer membrane lipopolysaccharide is directly available for attack. However, HEC_m-g-$P(IL)_{10}$ with lower graft densities (m =0.3 and 0.17) have similar antibacterial effects against both bacteria (*E. coli* and *S. aureus*) and this could be due to relatively good accessibility of the cationic charge to destabilise readily Gram-positive bacteria. The graft copolymers

therefore display promising antibacterial properties which could extend the use of cellulosic materials in a variety of applications.

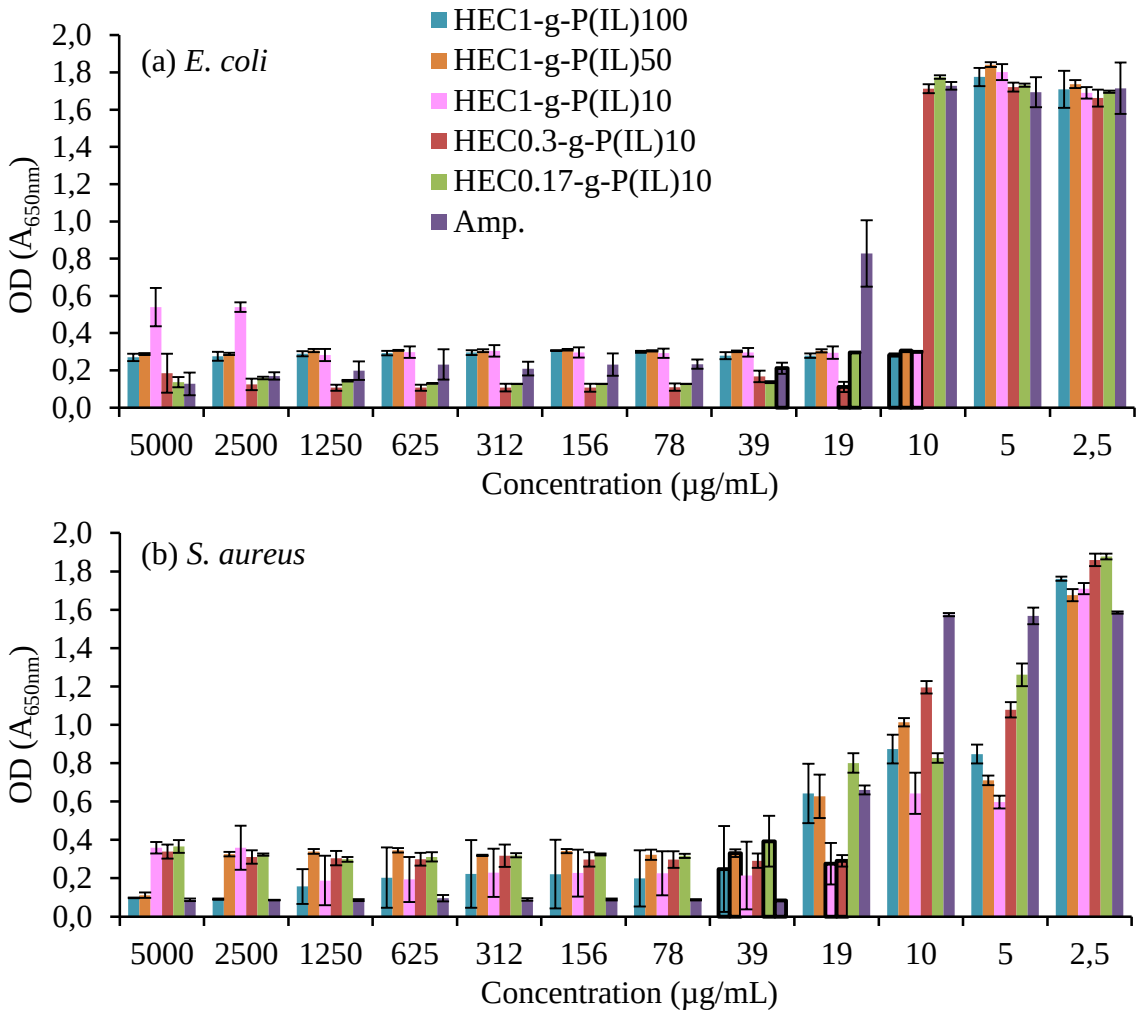

Figure 9. Determination of the MIC of HEC-g-P(IL)s for: (a) *E. coli* and (b) *S. aureus.* The MIC for each graft polymer is indicated.

3.2.2. Cytotoxicity

To evaluate the possible use of HEC_m-g-$P(IL)_n$s in medical applications, an estimation of cytotoxicity was essential. Cytotoxicity is measured using LD_{50}, the lethal dose that kills 50% of cells. An immortalized lung alveolar cell line (A549) was used. A 500 µg/mL concentration solution was prepared for each graft copolymer followed by 11 x 2-fold serial dilutions. Each solution was spotted into a 96-well plate containing the cells. After incubating overnight, Almar blue solution was added and the fluorescence of each well containing both cells and HEC-g-P(IL) was determined. The evolution of fluorescence intensity as a function of the concentration of each graft copolymer is displayed in Figure 10.

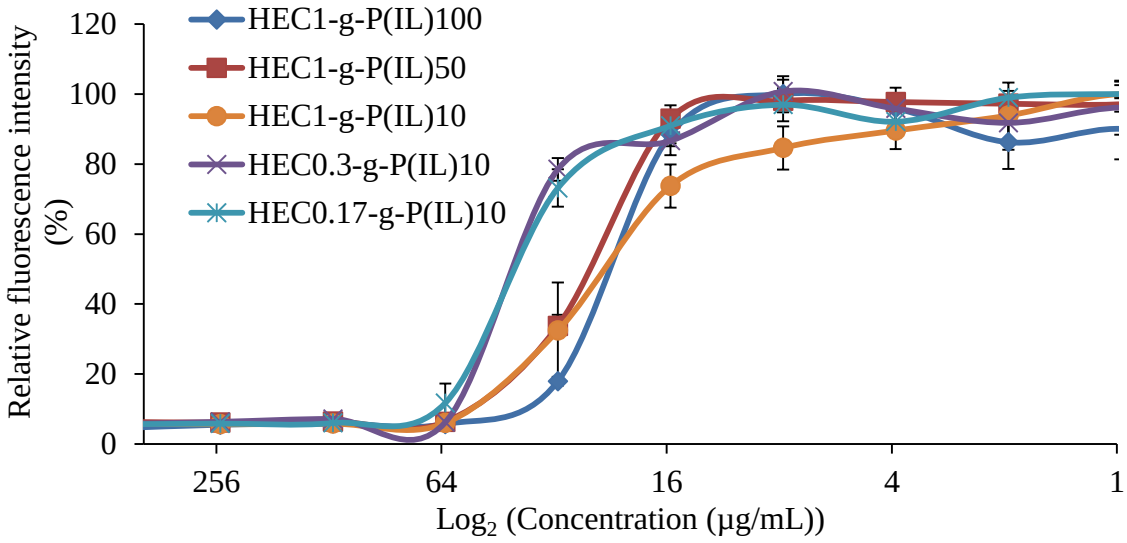

Figure 10. Determination of LD_{50} for HEC-g-P(IL)s.

The fluorescence decreases with the death of the cells and approaches zero when all cells have died, however, LD_{50} corresponds to the concentration of HEC-g-P(IL) at which half of the

fluorescence was lost. For HEC_1-g-$P(IL)_n$s (n =10, 50 and 100), LD_{50} was ~25 µg/mL whereas ~45 µg/mL LD_{50} was measured for HEC_m-g-$P(IL)_{10}$s (m =0.3 and 0.17). The chain length did not significantly influence the toxicity of the graft copolymers, however, a decrease of the graft density of $P(IL)_{10}$ onto HEC reduced the toxicity of the graft copolymers towards the cells. The cationic charge is responsible for the attachment between the cell membrane and the graft copolymers resulting in the necrosis of the cell, i.e. their death[35, 36]. One plausible reason of the reduction of the toxicity observed when decreasing the graft density is the decrease of the number of cationic charges on the outer surface of the graft copolymers. The LD_{50} values were similar to the MIC values, indicating that the doses required to inhibit the growth of the bacteria are close to those that kill 50% of the cells.

4. CONCLUSION

Graft copolymers of HEC and a poly(ionic liquid) (P(IL)) were successfully prepared using a versatile method combining RAFT polymerisation and CuAAC. P(IL)s **11** with different DPs (10, 50 and 100) were synthesised with monomer conversions up to ~80% using a xanthate as a chain transfer agent. The dispersity of $P(IL)_{100}$ was measured using SEC and was found to be ~1.5. P(IL)s were further coupled to azido-functionalized HEC **2**, which was prepared via the full functionalization of the primary alcohols of HEC with sodium azide. This produced graft copolymers having both different chain lengths of $P(IL)_n$ (n =10, 50 and 100) per AGU unit and different graft densities of $P(IL)_{10}$ onto HEC_m (m =0.3 and 0.17; i.e. 1 chain of $P(IL)_{10}$ per 3 or 6 AGU units). Subsequently, the graft copolymers were characterised using (^{13}C and ^{15}N) CP-MAS NMR and FT-IR spectroscopies. The observed decrease of the graft density of $P(IL)_{10}$ onto

HEC provided evidence of the success of the "click" reaction. Antibacterial properties of the graft copolymers were evaluated against *E. coli* (Gram-negative) and *S. aureus* (Gram-positive) and were comparable to those of a commonly employed antibiotic, ampicillin. For HEC_1-g-$P(IL)_n$ (n =10, 50 and 100), the minimum inhibition concentration (MIC) against *E. coli* was the same (10 μg/mL) indicating no influence of the chain length, however, a decreased graft density reduced the inhibitory effect (MIC =19 μg/mL) of $HEC_{0.3}$-g-$P(IL)_{10}$ and $HEC_{0.17}$-g-$P(IL)_{10}$. This suggests that the antibacterial properties arise from the number of cationic charges on the outer surface of the graft copolymers. For the Gram-positive bacterium (*S. aureus*), higher MICs were obtained indicating weaker inhibitory effects of the graft copolymers as compared to *E. coli*, potentially because of their different cell envelopes. However, the shortest chain length (n =10) had a slightly stronger inhibitory effect (MIC =19 μg/mL) compared to graft copolymers with a longer graft chain length (MIC =39 μg/mL) possibly because of higher accessibility of the cationic charge due to the limitation of the conformational flexibility. Furthermore, a decrease of the graft density of HEC_m-g-$P(IL)_{10}$ to 0.3 did not affect the antibacterial properties, however, a further decrease to 0.17 reduced the inhibitory effect to a value comparable to those of HEC_1-g-$P(IL)_n$ (n =100 and 50). This is most likely due to the considerable decrease of the number of cationic charges on the outer surface. To evaluate the potential of this antibacterial HEC graft copolymer, the cytotoxicity was evaluated using LD_{50} measurements. Values close to the MIC values were found consistent with toxicity due to membrane damage in both the prokaryotic and eukaryotic cells tested here. This suggests that these HEC-g-P(IL) graft copolymers are most likely to be appropriate for use as antibacterial coatings.

Supporting Information

The Supporting Information includes a scheme for the synthesis of the chain-transfer agent xanthate, the reaction conditions of the RAFT polymerisations of the ionic liquid monomer and the reaction conditions of the "click" reaction between P(IL) and N_3-HEC. This material is available free of charge via the Internet at http://pubs.acs.org.

Acknowledgements

We thank Dr David Apperley and other staff members of the EPSRC solid state NMR National Facility at Durham University for their assistance.

Author Contributions

The manuscript was written through contributions of all authors. All authors have given approval to the final version of the manuscript.

Funding sources

We thank EPSRC and Ashland Inc. for financial support (studentship to FJ).

Conflict of Interest Disclosure

Dr Osama Musa is an employee of Ashland Inc., which is a producer of hydroxyethyl cellulose.

References

1. Klemm, D.; Schmauder, H.-P.; Heinze, T. Cellulose. In *Biopolymers Online*; Steinbüchel, A., Eds.; Wiley-VCH Verlag GmbH & Co. KGaA, 2005.

2. D. R. Nobles, Jr.; R. M. Brown, Jr., *Cellulose* **2008,** *15,* 691-701.

3. *Polysaccharides: Structural Diversity and Functional Versatility*; Dumitriu, S. E., Eds.; Marcel Dekker: New York, 2005.

4. O'Sullivan, A. *Cellulose* **1997,** *4,* 173-207.

5. *Biopolymers: New Materials for Sustainable Films and Coatings*; Plackett D. E., Eds.; John Wiley & Sons: Chichester, 2011.

6. Kamel, S.; Ali, N.; Jahangir, K.; Shah S. M.; El-Gendy, A. A. *Express Polym. Lett.* **2008**, *2,* 758-778.

7. *Cork: Biology, Production and Uses*; Pereira, H., Eds.; Elsevier: Amsterdam, 2007.

8. Tashiro, T. *Macromol. Mater. Eng.* **2001,** *286,* 63-87.

9. Muñoz-Bonilla, A.; Fernández-García, M. *Prog. Polym. Sci.* **2012,** *37,* 281-339.

10. Gilmore, B. F.; Andrews, G. P.; Borberly, G.; Earle, M. J.; Gilea, M. A.; Gorman, S. P.; Lowry, A. F.; McLaughlin, M.; Seddon, K. R. *New J. Chem.* **2013,** *37,* 873-876.

11. Demberelnyamba, D.; Kim, K.-S.; Choi, S.; Park, S.-Y.; Lee, H.; Kim C.-J.; Yoo, I.-D. *Bioorg. Med. Chem.* **2004,** *12,* 853-857.

12. Cole, M. R.; Li, M.; El-Zahab, B.; Janes, M. E.; Hayes D.; Warner, I. M. *Chem. Biol. Drug Des.* **2011,** *78,* 33-41.

13. Yuan, J.; Antonietti, M. *Polymer* **2011,** *52,* 1469-1482.

14. Ding, S.; Tang, H.; Radosz, M.; Shen, Y. *J. Polym. Sci., Part A: Polym. Chem.* **2004,** *42,* 5794-5801.

15. He, H.; Zhong, M.; Luebke, D.; Nulwala H.; Matyjaszewski, K. *J. Polym. Sci., Part A: Polym. Chem.* **2014,** *52,* 2175-2184.

16. Ma, X.; Ashaduzzaman, M.; Kunitake, M.; Crombez, R.; Texter, J.; Slater L.; Mourey, T. *Langmuir* **2011,** *27,* 7148-7157.

17. Mori, H.; Yahagi M.; Endo, T. *Macromolecules* **2009,** *42,* 8082-8092.

18. Vijayakrishna, K.; Jewrajka, S. K.; Ruiz, A.; Marcilla, R.; Pomposo, J. A.; Mecerreyes, D.; Taton D.; Gnanou, Y. *Macromolecules* **2008,** *41,* 6299-6308.

19. *Advances in Food Research*, Stewart, G. F. E., Mrak, E. M., Chischester C. O., Eds.; Academic Press: London, 1963.

20. *Coatings Materials and Surface Coatings*; Tracton, A. A., Eds.; CRC Press: , 2006.

21. *Controlled Release in Oral Drug Delivery*; Wilson, C. G., Crowley, P. J., Eds.; Springer: London, 2011.

22. Joubert, F.; Musa, O.; Hodgson, D. R. W.; Cameron, N. R. *Polym. Chem.* **2015,** *6,* 1567-1575.

23. Eissa, A. M.; Khosravi, E.; Cimecioglu, A. L. *Carbohydr. Polym.* **2012,** *90,* 859-869.

24. Akeroyd, N.; Pfukwa, R.; Klumperman, B. *Macromolecules* **2009,** *42,* 3014-3018.

25. Harmand, J.; Rogalski, M.; Sindt, M.; Mieloszynski, J.-L. *Environ. Chem. Lett.* **2009,** *7,* 255-260.

26. Hayashi, K.; Morooka, N.; Yamamoto, Y.; Fujita, K.; Isono, K.; Choi, S.; Ohtsubo, E.; Baba, T.; Wanner, B. L.; Mori H.; Horiuchi, T. *Mol. Syst. Biol.* [Online] **2006,** DOI: 10.1038/msb4100049. http://msb.embopress.org/content/msb/2/1/2006.0007.full.pdf (accessed Oct 29, 2015)

27. Rosenbach, F. I. *Mikroorganismen Bei Den Wund-Infections- Krankheiten Des Menschen*, Bergmann, J. F., Eds.; Wiesbaden, 1884.

28. Andrews, J. M. *J. Antimicrob. Chemother.* **2001,** *48,* 5-16.

29. Lieber, M.; Smith, B.; Szakal, A.; Nelsonrees, W.; Todaro, G. *Int. J. Cancer* **1976,** *17,* 62-70.

30. Andreas, B. Patent CA 2089870, 1993.

31. Corredor, M.; Bujons, J.; Messeguer, A.; Alfonso, I. *Org. Biomol. Chem.* **2013,** *11,* 7318-7325.

32. Wrackmeyer, B. *Z. Naturforsch. B.* **2011,** *66,* 1079-1082.

33. Lyčka, A.; Doleček, R.; Šimûnek, P.; Macháček, V. *Magn. Reson. Chem.* **2006,** *44,* 521-523.

34. Silhavy, T. J.; Kahne, D.; Walker, S. *Cold Spring Harbor Perspect. Biol.* [Online] **2010**, DOI: 10.1101/cshperspect.a000414. http://cshperspectives.cshlp.org/content/2/5/a000414.full.pdf+html (accessed Oct 29, 2015)

35. Lu, G.; Wu, D.; Fu, R. *React. Funct. Polym.* **2007,** *67,* 355-366.

36. Fischer, D.; Li, Y.; Ahlemeyer, B.; Krieglstein, J.; Kissel, T. *Biomaterials* **2003,** *24,* 1121-1131.

Table of Contents Graphic